

M.B. Gay Ducati ^{1,†}, V.P. Gonçalves ^{2,*}, M.V.T. Machado ^{1,★}¹ *Instituto de Física, Universidade Federal do Rio Grande do Sul
Caixa Postal 15051, CEP 91501-970, Porto Alegre, RS, BRAZIL*² *Instituto de Física e Matemática, Universidade Federal de Pelotas
Caixa Postal 354, CEP 96010-090, Pelotas, RS, BRAZIL*

The logarithmic slope of diffractive structure function is a potential observable to separate the hard and soft contributions in diffraction, allowing to disentangle the QCD dynamics at small x region. In this paper we extend our previous analyzes and calculate the diffractive logarithmic slope for three current approaches in the literature: (i) the Bartels-Wusthoff model, based on perturbative QCD, (ii) the CKMT model, based on Regge theory and (iii) the Golec Biernat - Wusthoff model which assumes that the saturation phenomena is present in the HERA kinematic region. We analyze the transition region of small to large momentum transfer and verify that future experimental results on the diffractive logarithmic slope could discriminate between these approaches.

12.38.Aw; 12.38.Bx; 13.60.Hb

I. INTRODUCTION

Recent measurements of the structure functions for the deep inelastic ep scattering at HERA has probed the interface between hard and soft physics in the description of strong interactions. While the perturbative QCD DGLAP evolution [1] describes very well the experimental results at medium x and high Q^2 (respectively, the momentum fraction carried by the partons and the momentum transfer), the description of data at small values of x is a particularly rich and complex subject in which the usual approach meets and competes with distinct approaches, some based on QCD, others on Regge theory or essentially *ad hoc* phenomenological models (For a review see e.g. Ref. [2]). Basically these approaches describe very well the proton structure function data, which implies a theoretical and experimental challenge: the derivation of a quantity which allows us to disentangle the hard and soft contributions for the dynamics at small x . Recently, we have proposed the analyzes of the slope of diffractive structure function as a potential observable to explicit the leading dynamics at ep diffractive processes [3]. Here we study in detail the predictions for this quantity for three current approaches present in the literature, which describe very well the HERA data. Before to present our results, we discuss the motivation of our work.

About two years ago, the measurement at HERA ep collider of the logarithmic slope (Q^2 -slope) of the inclusive structure function $F_2(x, Q^2)$ has presented a new challenge for the small x regime [4,5]. Basically, the turn over of the Q^2 -slope was initially considered as an evident signal for the change of the dynamics, namely a transition from the perturbative QCD to the high density regime (e.g., see Ref. [6]). However, adjustments in the usual parton distribution functions (pdf's) allow to extend the DGLAP formalism to be valid in lower momentum transfer values [7,8] ($Q^2 \leq 3$ GeV² and Bjorken variable $x < 5 \cdot 10^{-3}$), with a reasonable description of the F_2 slope data. Furthermore, the HERA results have motivated the proposition of other approaches which consider the interplay between hard and soft physics. Essentially, we can separate these models in two categories: (a) the ones that assume the Regge framework as starting point at small x and Q^2 , and consider improvements to describe the large Q^2 region and, (b) those that assume the validity of pQCD at large Q^2 and estimate the perturbative corrections present at small x and Q^2 . Although at this moment we have distinct models, based on different assumptions, which reasonably describe the HERA data for F_2 and its slope, there is the expectation that future experimental results for the F_2 slope would allow to discriminate the correct dynamics at small x [9].

In a similar way as the $F_2(x, Q^2)$ case, the logarithmic slope of the diffractive structure function should be studied and its role to disentangle the dynamics (soft and/or hard) needs investigation, since at present there exists enough statistics in the $F_2^{D(3)}(x_P, \beta, Q^2)$, the diffractive structure function, experimental measurements to obtain data for this

[†] E-mail: gay@if.ufrgs.br

^{*} E-mail: barros@ufpel.tche.br

[★] E-mail: magnus@if.ufrgs.br

quantity. In the kinematic domain of the present experimental measurements, x_P may be interpreted as the fraction of the four-momentum of the proton carried by the diffractive exchange, the Pomeron, if such a picture is invoked. Moreover, β is the fraction of the four-momentum of the diffractive exchange carried by the parton interacting with the virtual boson. Theoretically, when we look into diffractive dissociation in deep inelastic scattering (DDIS), mainly on F_2^D , the interplay between hard and soft regimes is more explicit [10,11]. Basically, the partonic fluctuations of the virtual photon can lead to configurations of different sizes when analyzed in the proton rest frame. The study of the diffractive dissociation of protons has shown that for real photons ($Q^2 \approx 0$), where the transverse size of the incoming pair is approximately that of a hadron, the energy dependence is compatible with the expectations based on the soft Pomeron exchange. On the other hand, at large Q^2 the energy dependence is higher than that of the soft Pomeron, suggesting that pQCD effects may become visible for small incoming quark-antiquark pairs. Therefore, as the F_2^D structure function is inclusive to the hard and soft contributions to the dynamics, the analyzes of its logarithmic slope is maybe a better test for the Pomeron physics.

First, we consider a Regge inspired model [12,13], where the diffractive production is dominated by the soft (non-perturbative) Pomeron. In this framework, the correspondent diffractive structure function is connected with the inclusive one and a particular expression to the Pomeron flux has been used. In a second step, one takes into account a pQCD approach [14], where the diffractive process is modelled as the scattering of the photon Fock states ($q\bar{q}$ and $q\bar{q}$ +gluon configurations) with the proton through the color singlet two hard gluon exchange (in the proton rest frame). Moreover, we calculate the F_2^D -logarithmic slope considering the phenomenological saturation model from Ref. [15] and perform a comparison with the previous non-saturated approach [14], pointing out their main differences. We found that these different approaches predict very distinct behaviors for the logarithmic slope, which may shed light into the leading dynamics at ep diffractive processes if this quantity is experimentally analyzed.

The paper is organized as follows. In the next section we present the basic formulae and a very brief review of two distinct frameworks for the diffractive structure function: the Capella et al. (Regge framework) approach without Q^2 evolution, and the Bartels-Wüsthoff model considering its phenomenological parameterization (pQCD-based). Moreover, in this section we derive the expressions for the F_2^D -logarithmic slope. In the Sec. III the correspondent predictions to the F_2^D logarithmic slope from these models are presented and discussed. The saturation phenomena is addressed in Sec. IV, where we show the results for both saturated and non-saturated pQCD approaches. In the last section we draw our conclusions.

II. DIFFRACTIVE DIS AND PHENOMENOLOGICAL APPROACHES

A. The Regge inspired model

Considering diffractive (Ingelman-Schlein) factorization [16], the probe of the virtual photon in DIS provides understanding on the nature of the Pomeron and the partonic structure of that object. A few years ago Capella-Kaidalov-Merino-Tran Thanh Van (CKMT) proposed a model to diffractive DIS based on Regge theory [12,13] and the Ingelman-Schlein ansatz. In this case, deep inelastic diffractive scattering proceeds in two steps (the Regge factorization): first a Pomeron is emitted from the proton and then the virtual photon is absorbed by a constituent of the Pomeron, in the same way as the partonic structure of the hadrons.

The Pomeron is considered as a Regge pole with a trajectory $\alpha_P(t) = \alpha_P(0) + \alpha' t$ determined from soft processes, in which absorptive corrections (Regge cuts) are taken into account. Explicitly, $\alpha_P = 1.13$ and $\alpha'_P = 0.25 \text{ GeV}^{-2}$. The diffractive contribution to DIS is written in the factorized form:

$$F_2^D(x, Q^2, x_P, t) = \frac{[g_{pp}^D(t)]^2}{16\pi} x_P^{1-2\alpha_P(t)} F_P(\beta, Q^2, t), \quad (1)$$

where the details about the coefficients appearing in the Pomeron flux can be found in Ref. [13].

Moreover, F_P is determined using Regge factorization and the values of the triple Regge couplings obtained from soft diffraction data. Namely, the Pomeron structure function is extracted from F_2^P , or more precisely from the combination $F_2^d = \frac{1}{2}(F_2^p + F_2^n)$, by replacing the Reggeon-proton couplings by the corresponding triple reggeon couplings (see Ref. [12]). One of the main points of this model is the dependence on Q^2 of the Pomeron intercept [$F_P \propto \beta^{\Delta(Q^2)}$]. For low values of virtuality (large cuts), Δ is close to the effective value found from analyzes of the hadronic total cross sections ($\Delta \sim 0.08$), while for high values of Q^2 (small cuts), Δ takes the bare Pomeron value, $\Delta \sim 0.2 - 0.25$.

The comparison of the CKMT model with data is quite satisfactory, mainly when considering a perturbative evolution of the Pomeron structure function. We notice that here one uses the pure CKMT model [12] rather than including QCD evolution of the initial conditions [13], which has been considered to improve the model at higher

Q^2 . Such procedure ensures that we take just a strict Regge model, namely avoiding contamination by pQCD phenomenology.

Justifying our choice, the CKMT model is a long standing approach describing in a consistent way both inclusive and diffractive deep inelastic based on Regge theory, which is continuously improved considering updated experimental results [17]. In general, Regge inspired approaches focus only the inclusive case, or exclusively diffractive DIS. A subtle question concerning the CKMT approach is the dependence of the Pomeron intercept on the virtuality in the inclusive case. Although the need of this Q^2 -dependence, claimed by Kaidalov for a long time (for a review see [18]), the smooth interpolation between a soft and a semihard intercept seems to break off the pure reggeonic feature of the model. However, in diffractive deep inelastic the energy dependence (i.e., the Pomeron flux) is driven by a soft Pomeron with a fixed $\alpha_P = 1.13$, properly corrected by absorptive effects. Indeed, this fact is verified at our previous work [3], when considering the effective slope $\partial \ln F_2^D / \partial \ln(1/x_P)$. We notice that here one uses the pure CKMT model [12] rather than including QCD evolution of the initial conditions [13], which has been considered to improve the model at higher Q^2 . Such procedure ensures that we take just a Regge model, namely avoiding contamination by pQCD phenomenology.

Considering all properties of the diffractive structure function on the CKMT model, the calculation of the logarithmic slope is straightforward. The expression reads now:

$$\frac{dF_2^D}{d \ln Q^2} = \mathcal{N} x_P^{1-2\alpha_P(0)} \left[eA \beta^{-\Delta(Q^2)} (1-\beta)^{n(Q^2)+2} \left(\frac{Q^2}{Q^2+a} \right)^{1+\Delta(Q^2)} S_P(Q^2, \beta) + \right. \\ \left. fB \beta^{1-\alpha_R} (1-\beta)^{n(Q^2)-2} \left(\frac{Q^2}{Q^2+b} \right)^{\alpha_R} S_R(Q^2, \beta) \right], \quad (2)$$

where the overall normalization \mathcal{N} comes from the integration over t of the Pomeron flux, $n(Q^2) = \frac{3}{2} \left(1 + \frac{Q^2}{Q^2+c} \right)$, α_R is the secondary reggeon intercept (CKMT supposes that the only secondary trajectory that contributes is the f one). The coefficients and constants are taken from Ref. [13]. Moreover, the factors $S_{P,R}(Q^2, \beta)$ are defined as

$$S_P(Q^2, \beta) = \Delta(Q^2) \left[\frac{a}{Q^2+a} \right] + \frac{3c}{2} \left[\frac{Q^2}{(Q^2+c)^2} \right] \ln(1-\beta) + \\ + 2d\Delta_0 \left[\frac{Q^2}{(Q^2+d)^2} \right] \ln \left(\frac{Q^2}{\beta(Q^2+a)} \right), \quad (3)$$

$$S_R(Q^2, \beta) = \alpha_R(0) \left[\frac{b}{Q^2+b} \right] + \frac{3c}{2} \left[\frac{Q^2}{(Q^2+c)^2} \right] \ln(1-\beta). \quad (4)$$

The above expressions have been used in our previous work [3] to obtain the main features of this model concerning the F_2^D -logarithmic slope, analyzing the x_P , β and Q^2 spectra under a kinematical constraint which relates the variables x and Q^2 . In the next section we will present a brief review of the results from Ref. [3] and a full analyzes of this quantity when the kinematic constraint is not assumed. Before, however, we present the derivation of the F_2^D slope in the pQCD approach.

B. The perturbative QCD approach

Although the diffractive dissociation is mainly connected to soft processes and thus linked with the Regge theory, the pQCD framework has been recently used by some authors to describe quite well the diffractive structure function [19,20]. The main properties of the pQCD models are very similar. In particular, we consider for our analyzes the Bartels-Wusthoff model and its further parameterization to the measurements [14]. The physical picture is that, in the proton rest frame, diffractive DIS is described by the interaction of the photon Fock states ($q\bar{q}$ and $q\bar{q}g$ configurations) with the proton through a Pomeron exchange, modeled as a two hard gluon exchange. The corresponding structure function contains the contribution of $q\bar{q}$ production to both the longitudinal and the transverse polarization of the incoming photon and of the production of $q\bar{q}g$ final states from transverse photons. The basic elements of this approach are the photon light-cone wave function and the non-integrated gluon distribution (or dipole cross section in the dipole formalism). For elementary quark-antiquark final state, the wave functions depend on the helicities of the photon and of the (anti)quark. For the $q\bar{q}g$ system one considers a gluon dipole, where the $q\bar{q}$ pair forms an effective gluon state associated in color to the emitted gluon and only the transverse photon polarization is important. The interaction with the proton target is modeled by two gluon exchange, where they couple in all possible combinations to the dipole.

In a comparison with data, the transverse $q\bar{q}$, $q\bar{q}g$ production and the longitudinal $q\bar{q}$ production dominate in distinct regions in β , namely medium, small and large β respectively [14]. The β spectrum and the Q^2 -scaling behavior follow from the evolution of the final state partons, and are derived from the light-cone wave functions of the incoming photon, decoupling from the dynamics inside the Pomeron, while the energy dependence and the normalizations are free parameters.

The calculation of the expression for the F_2^D -logarithmic slope is straightforward, considering each contribution coming from the different configurations of the photon Fock state. Moreover, this approach allows to obtain parameter free predictions for the logarithmic slope, since all parameters have been obtained in comparison with the H1 and ZEUS data. We justify our choice due to the simple analytic expressions for the diffractive structure function for each Fock state configuration which turn out to be the clearest and avoiding cumbersome numeric calculations.

The explicit expressions for the diffractive logarithmic slope are written as

$$\begin{aligned} \frac{d F_2^{D(3), q\bar{q}T}(x_P, \beta, Q^2)}{d \ln Q^2} &= \frac{n_2^1}{(\ln \frac{Q^2}{Q_0^2} + 1)} F_2^{D(3), q\bar{q}T}(x_P, \beta, Q^2) , \\ \frac{d F_2^{D(3), q\bar{q}G}(x_P, \beta, Q^2)}{d \ln Q^2} &= \frac{1}{(\ln \frac{Q^2}{Q_0^2} + 1)} \left[n_2^1 + \frac{Q^2}{Q^2 + Q_0^2} \right] F_2^{D(3), q\bar{q}G}(x_P, \beta, Q^2) , \\ \frac{d F_2^{D(3), q\bar{q}L}(x_P, \beta, Q^2)}{d \ln Q^2} &= \left[\frac{n_4^1}{(\ln \frac{Q^2}{Q_0^2} + 1)} + \frac{Q^2 - 7 \beta Q_0^2}{Q^2 + 7 \beta Q_0^2} \right] F_2^{D(3), q\bar{q}L}(x_P, \beta, Q^2) . \end{aligned} \quad (5)$$

The expressions of the distinct contributions to $F_2^{D(3)}$ can be found in Ref. [14], as well as the remaining parameters.

The above expressions describe the x_P , β and Q^2 behavior of the F_2^D -logarithmic slope in the pQCD model. In next section we present a brief review of the main conclusions from Ref. [3] and extend our analyzes for the case where a kinematical constraint is not assumed.

III. THE F_2^D LOGARITHMIC SLOPE FROM REGGE AND PQCD-BASED APPROACHES

Before we perform the analyzes of the presented models, some comments are in order. In the first extraction of the F_2 slope data at HERA, the so-called Caldwell plot [4], the variables x and Q^2 were strongly correlated. For a limited acceptance (in the case of the latest HERA F_2 -slope data) and for a fixed energy, one always has a limited range in Q^2 at any given x , with average $\langle Q^2 \rangle$ becoming smaller for smaller x . The latest measurements of the F_2 -slope presents an increase when x decreases down to $\sim 10^{-4}$, and then a turn over appears, with a slope decreasing at lower x (or Q^2) values. This peak is currently interpreted as a transition region from a perturbative QCD regime to a Regge behavior and the maximum is related to the correlation between the kinematical variables mentioned above.

From the theoretical point of view however, the logarithmic slope depends on two variables (x and Q^2) which are independent and one is not restricted to follow a particular path on the surface representing the Q^2 -slope. However, to perform a comparison with those data, due to low statistics, we should connect x and Q^2 by some analytical dependence $Q^2 = Q^2(x)$ that lies within a physical region on (x, Q^2) -plane. This region is bounded by the condition

$$y = \frac{Q^2}{x(s - m_p^2)} \leq 1 . \quad (6)$$

For the HERA experiments, the centre of mass energy is $\sqrt{s} \approx 300$ GeV and this condition writes $Q^2 < 9.10^4 x$. An usual procedure is to perform a fit to the (x, Q^2) -plane satisfying the above condition. In the previous work [3], one considers the path used by the MRST99 group [8] in their analyzes of the F_2 -logarithmic slope, $Q^2 = 1280 x^{0.705}$ (for H1 slope data). We take this into account because, concerning the F_2^D -slope, in a first trial study probably we should expect a poor statistics in a similar way as it was for the inclusive case [4].

In Fig. 1 one shows the quantity $dF_2^{D(3)}/d \ln(Q^2)$ (shortly, Q^2 -slope) versus x_P at β typical values, considering the kinematical constraint discussed above. Due to the kinematical constraint we show the results at $\beta=0.04, 0.1, 0.4$ and 0.9 starting at $x_P = 10^{-3}$, meaning virtualities $Q^2 > 1$ GeV² (in which the pQCD model is valid). We also do not consider the introduction of reggeonic contributions, which are important at low β (larger x_P).

We found that the CKMT model (without Q^2 evolution) provides a transition between positive and negative slope values at $\beta = 0.4$, when considering the x_P dependence. This behavior is consistent since the Pomeron structure function in this model is related to the nucleon structure function F_2 , which presents that feature due to the scaling

violation. Moreover, in Ref. [3] we have verified that the β dependence, at $x_P \geq 10^{-3}$, is predominantly flat on the whole kinematic range of β and it has a turn over in $\beta = 0.1$ at $x_P = 10^{-4}$. Since the Pomeron structure function in the CKMT is just the inclusive structure function F_2 , the large value of the slope at small β (corresponding to the Bjorken x in inclusive DIS) was expected, as well as the presence of a similar turnover found in the first measurements of the inclusive structure function slope. Considering the DGLAP evolution [13], we would expect a Q^2 -slope close to zero at $\beta = 0.65$ and even negative at $\beta = 0.9$. An important point is the faster decreasing of CKMT at large β , coming from the logarithmic factors $S_{P,R}(Q^2, \beta)$. Furthermore, the CKMT model predicts a constant x_P -slope. This fact comes from the choice of the Pomeron flux, which does not present an effective intercept depending on virtuality Q^2 , contrasting with the inclusive case where the intercept smoothly interpolates the soft and semi-hard regions. Further, we return to the analyzes of the CKMT model, disregarding the kinematical constraint, in explicit comparison with the pQCD approach reviewed in the subsection (IIB).

Concerning the pQCD model, we have that the slope is predominantly positive in almost all considered β , taking negative values only at $\beta = 0.9$ for the interval $x_P < 0.0004$. As shown in Ref. [3], the slope presents a β dependent turn over, which is shifted to greater x_P values as β increases. The positive behavior of the slope at low values of β is associated to the $q\bar{q}G$ contribution, while for intermediate β the $q\bar{q}T$ state dominates, producing an almost constant function on Q^2 . The high β behavior is consistent with the H1 measurements, in the region $x_P > 10^{-3}$, which prefer a positive slope in Q^2 , corresponding to a large $q\bar{q}G$ contribution in this region [14]. Furthermore, we have shown that the β dependence, at $x_P \geq 10^{-3}$, is predominantly flat on the whole kinematic range of β and it has a turn over at $\beta = 0.5$ and $x_P = 10^{-4}$. Moreover, this model gives a x_P -slope dependent on both the virtuality Q^2 and β . The virtuality dependence is clear from the parametrization on the energy, constructed to interpolate between a softer effective intercept at low Q^2 up to semihard values at higher virtualities. The hard-like value of the intercept at higher β is a feature already discussed in Refs. [14].

Confronting the approaches, we conclude in [3] that both models predict a positive slope up to $\beta \sim 0.4$, with a steeper decreasing in CKMT. The high β region discriminates the behaviors. The pQCD results provide a positive slope, while CKMT produces negative values. This comes from the fact that the CKMT approach does not include the $q\bar{q}G$ contribution, which is dominant in this region (small x_P and Q^2) for the pQCD model. The Q^2 -behavior in the CKMT is determined by the F_2 scaling violations, including only the $q\bar{q}_{T,L}$ contributions.

In Figs. 2-3 we present a new comparison between the models, without imposing a kinematical constraint. In Fig. 2 one shows the β -dependence for typical values of x_P and Q^2 , where the momentum transfer is ranging from 1 up to 100 GeV^2 . The CKMT model predicts a flat behavior on the whole β range. Particularly, at $Q^2 = 1 \text{ GeV}^2$ there is a strong decreasing of the slope at large β . This is due to the presence of factors $\ln(1 - \beta)$ in the second terms of Eqs. (3-4). For larger Q^2 values, the logarithm on Q^2 , namely the third term of Eq. (3), compensates the decreasing. At momentum transfer of 100 GeV^2 , the CKMT predicts a flat behavior of the slope into all β spectrum. The pQCD model produces an increasing of the slope in both small and large values of β , while presents a flat behavior at the medium one. These increasing on the slope are due to the enhancements in the $q\bar{q}G$ (dominant at low β) and $q\bar{q}L$ (leading at high β) contributions from the Q^2 -factors appearing in Eq. 5 ($q\bar{q}G$ and $q\bar{q}L$), respectively. A steep Q^2 -slope decreasing into negative values is also present at the virtuality $Q^2 = 1 \text{ GeV}^2$ for large β , in a similar way to the CKMT model. However, beyond the contribution of the (dominant) longitudinally polarized $q\bar{q}$ pair configuration, this region also receives contributions associated to the $q\bar{q}G$ configuration, as discussed above.

In Fig. 3 one presents the x_P dependence at medium and large β . The low β region was disregarded in order to avoid to deal with subleading reggeonic contributions, important in this kinematical domain. We observe again a smooth behavior for the pQCD predictions, with a positive slope in almost the whole range (negative values are present at both large β and $Q^2 = 1 \text{ GeV}^2$, in agreement with the discussion in the previous paragraph). The CKMT model predicts predominantly negative slope values in this kinematical domain, converging to a flat value for larger x_P . A clear difference between the predictions of the two models is the change of signal of the slope with the Q^2 evolution at medium β present in the CKMT prediction. Those behaviors are also consistent with the previous plots using the kinematical constraint.

In summary, the results above should allow to discriminate the behaviors predicted from the different approaches, namely perturbative QCD (hard physics) and non-perturbative (soft) physics. Theoretically, this difference comes from the ansatz for the photon-proton interaction (hard or soft) and also from the relation of the Pomeron structure with the inclusive structure function used in the CKMT model. This relation implies the inclusion at most of the $q\bar{q}_T$ and $q\bar{q}_L$ configurations in the photon wave function in its estimates. On the other hand, the pQCD model analyzed here also includes the contribution of gluon emission in the photon wave function, which dominates at small β . Therefore, the analyzes of the β spectrum of the F_2^D slope would be important in an experimental studies. Moreover, concerning to the x_P spectrum, the signal of the slope at medium values of Q^2 ($Q^2 \approx 10 \text{ GeV}^2$) is a good search of information about the dynamics. In comparison with the experimental measurements of F_2^D , the results have favored the perturbative QCD framework [11].

In this section we take into account the saturation phenomena, considering its implications in the analyzes of the F_2^D -slope. The concept of saturation in DIS is connected to the transition in the underlying physical picture from high to low photon virtuality Q^2 , which is present in the measurements of the total γ^*p -cross section at HERA. From the theoretical point of view, saturation at low momentum fraction x occurs in the semi-hard region in which the parton density becomes quite high and the recombination effects tame the growth of the density [21]. As a consequence, the increasing of the total cross section is diminished at small x .

In perturbative QCD, in the proton rest frame, the γ^*p process is described in terms of the photon splitting into a quark-antiquark pair, far upstream of the nucleon, which then scatters in the proton [22] [For a review, see e.g. Ref. [23]]. In the perturbative regime this reaction is mediated by the one gluon exchange which turns out into a multi-gluon one when the saturation region is approached. A remarkable feature is that the mechanism leading to the photon dissociation and the further scattering has a factorizable form, written in terms of a convolution between a photon wave function and a quark-antiquark cross section [22]. The wave function to be calculated from perturbation theory, or the quark-antiquark cross section, so-called dipole cross section $\hat{\sigma}$, has a strong influence of the non-perturbative contributions and should be modeled. A review on issues concerning the modelling of the dipole cross section can be found in Ref. [24]. Here, we choose the saturation model from Ref. [15], which reproduces the experimental results at both inclusive and diffractive electroproduction.

Some comments about the saturation model are in order. Although this approach describes in very good agreement both DIS and diffractive dissociation, a more deep understanding of the underlying dynamics is far from clear. Namely, a connection with the gluon distribution function and the mechanism of unitarity control is needed (for a review of the current theoretical effort see, e.g., Ref. [25]). Moreover, the impact parameter dependence (b_t) of the process is not taken into account and the connection with DGLAP approach is missing (see criticisms to these points at [26]).

In that phenomenological approach, the dynamics of saturation is present in the effective dipole cross section, modelled in an eikonal way:

$$\hat{\sigma}(x, r^2) = \sigma_0 \left[1 - \exp \left(-\frac{r^2}{4 R_0^2(x)} \right) \right] , \quad (7)$$

where the x -dependent saturation scale (the saturation radius) is given by

$$R_0(x) = \frac{1}{Q_0} \left(\frac{x}{x_0} \right)^{\lambda/2} . \quad (8)$$

The normalization σ_0 and the parameters $x_0, \lambda > 0$ were determined from all inclusive data on $F_2(x, Q^2) \sim \sigma_T(x, Q^2)$ with $x < 10^{-2}$ [15]. The constant Q_0 sets the dimension. In summary, this phenomenological model consistently interpolates between the saturation regime and the scaling regime of $\sigma_T(F_2)$.

In order to calculate the logarithmic slope from the above approach, we should consider the diffractive structure function $F_2^{D(3)}$, which is given by [14]

$$F_2^D(x_P, \beta, Q^2) \sim \beta \int dt \int \frac{k_t^2 d^2 k_t}{(1-\beta)^2} \left| \int \frac{d^2 l_t}{l_t^2} D\Psi(\alpha, k_t) \mathcal{F}(l_t^2, k_0^2; x_P) \right|^2 , \quad (9)$$

where $D\Psi$ is a combination of the concerned wave functions, l_t is the transverse momentum of the exchanged gluons and $\mathcal{F}(l_t^2, k_0^2; x_P)$ defines the Pomeron amplitude (non-integrated gluon distribution). To take saturation into account, in Ref. [15] the unintegrated gluon distribution $\mathcal{F}(x, l_t^2)$ was calculated from the effective dipole cross section (the notation is the same of Sec. II B) as

$$\hat{\sigma}(x, r^2) = \frac{4\pi^2}{3} \int \frac{dl_t^2}{l_t^2} [1 - J_0(l_t r)] \alpha_s \mathcal{F}(x, l_t^2) , \quad (10)$$

with

$$\alpha_s \mathcal{F}(x, l_t^2) = \frac{3\sigma_0}{4\pi^2} R_0^2(x) l_t^2 e^{-R_0^2(x) l_t^2} . \quad (11)$$

The corresponding diffractive structure function is constructed summing three terms coming from the diffractive production of a quark-antiquark pair (photon polarized transverse and longitudinally) plus the contribution of the pair with emission of an additional gluon in the final state. The gluon emission is known only in certain approximations:

transverse (valid at very large virtualities and finite M_X) or longitudinal (at large M_X and finite virtualities) momenta components strongly ordered. This approach described above reproduces accurately the β and x_P distributions from the H1 and ZEUS data [2], with a free parameter description [15]. The main characteristic is the use of an universal non-integrated gluon distribution, modelled in a simple way to take into account the saturation phenomena and completely determined from the inclusive experimental data.

Now, having reviewed the main formulae concerning the phenomenological saturation model, we perform numerically the F_2^D logarithmic slope, using the same parameters from Ref. [15]. In this section we denote Q^2 -slope as the function $x_P dF_2^D/d\ln Q^2$. Since the $q\bar{q}G$ configuration dominates at small β , while the $q\bar{q}T$ one dominates at medium β and the $q\bar{q}L$ is important in the large β region, the behavior of the slope presents a strong dependence in this variable. In Fig. 4, we show the x_P dependence, considering typical β values and virtualities ranging from 1 up to 100 GeV². A remarkable fact is the presence of a transition between positive and negative slope signals, instead of a predominantly positive slope as in the non-saturated case. The transition is not present in the pQCD model without saturation due to the assumptions made in the parameterization of the HERA data in the region of large Q^2 (large β). It is important to emphasize that a transition is verified in the preliminary ZEUS analyzes of diffractive DIS [28], where the saturation model [15] is considered to describe the Q^2 dependence of the diffractive structure function, using as kinematical variables M_X and W rather than β and x_P . Such a procedure is performed due to the similarity of the behavior of $d\sigma/dM_X$ and $\sigma_{tot}(\gamma^*p)$ in the same kinematic range. In that analyzes, the growth of $x_P F_2^D$ versus Q^2 is stopped at $Q^2 \sim 10$ GeV² and has a smooth decreasing for larger virtuality values. The transition region corresponds to $\beta \sim 0.2$ for $M_X = 5$ GeV and $\beta \sim 0.07$ for $M_X = 11$ GeV.

In Fig. 5, one shows the x_P behavior for both approaches with [15] and without [14] saturation, at typical β values. We analyze in particular the transition region between hard and soft dynamics, settled by the low virtualities $Q^2 \sim 1.5 - 9$ GeV². The saturation model produces a transition between positive and negative slope values at low $\beta = 0.04$, while presents a positive slope for medium and large β . The pQCD approach without saturation, again shows a positive slope for the whole Q^2 and x_P range. Since the diffractive cross section is strongly sensitive to the infrared cutoff, one of the main differences between these models is the assumption related to the small Q^2 region. In the pQCD models without saturation, an ad hoc cutoff in the transverse momentum is inserted, as well as the energy dependence of the non-integrated gluon distribution. In the saturation model instead, the saturation radius $R_0(x)$ gives the infrared cutoff (the saturation momentum scale) and determines the energy dependence. If this scale is large (1-2 GeV²), then the resulting process is not soft and can be completely calculated using pQCD methods. Therefore, the saturation model extends the pQCD approach towards lower Q^2 values, making this region an important source of information about the dynamics. We conclude that, the difference between the behaviors predicted by these two models for the x_P spectrum, mainly in the region of small β and medium Q^2 , are large, which should allow to discriminate the dynamics in future experimental analyzes.

For completeness we mention that a hybrid approach for the saturation phenomena has been proposed recently mixing the multi-Pomeron exchange and concepts of pQCD, namely considering the configurations in Fock space of the virtual photon [29]. In that work the $q\bar{q}$ pair is separated in contributions of large size, described by "aligned jet" configuration, and contributions of short size driven by perturbative QCD as discussed in the previous sections. The gluon emission contribution is disregarded in this case. The multiple Pomeron exchange is taken into account considering a quasieikonal form for the cross sections written in impact parameter representation. Results for diffractive DIS are obtained since the multiple Pomeron exchanges are related by AGK-cutting rules to shadowing corrections to diffractive production. Such framework produces a good description of available experimental data from photo-production up to about 10 GeV². Their conclusions are similar to Ref. [15], namely the saturation effects at HERA energies are very important in the region of small Q^2 . However, unitarity corrections seem to appear at large Q^2 in [29] coming from the large size configuration and the triple Pomeron interaction. A direct comparison between the approaches from the Refs. [15] and [29] concerning the resultant F_2^D -slope is a interesting issue and it will be postpone to a future analyzes.

V. CONCLUSIONS

The study of electroproduction at small x has lead to the improvement of our understanding of QCD dynamics in the interface of perturbative and non-perturbative physics. However, many important problems remain unsolved. One of the main open questions is if the transition between large (pQCD) and small (Regge) virtualities is already reached or if a high density (saturation) regime is present. At this moment, there are several approaches, based in very distinct paradigms, which describe the current observables measured in HERA. In this paper we propose and analyze the diffractive logarithmic slope as a potential quantity to explicit the leading dynamics at ep diffractive processes. We study in detail the prediction for the logarithmic slope of the diffractive structure function, using three distinct models

for diffractive DIS. We choose as a pure Regge approach the CKMT model, which describes with quite good agreement the inclusive and diffractive structure function. The pQCD model used is a parametrization based on the Bartels-Wüsthoff approach, which describes successfully the diffractive DIS and other observables, like jet production. One analyzes was also performed for saturation phenomena, discussing the results from the phenomenological approach by Golec Biernat-Wüsthoff, describing its main features and comparison with the pQCD model without saturation. As a summary of our main results, we predict that: (a) the analyzes of the β spectrum in the region of small values of this variable and the signal of the slope in the x_P spectrum at medium Q^2 values should allow to discriminate between the Regge- and pQCD-based approaches; (b) The analyzes of the x_P spectrum of the slope at small values of β concerning to the Q^2 behavior should allow to discriminate between the saturated and non-saturated pQCD models.

A possible route to distinguish experimentally between the three models discussed in this paper is the following: (i) First, analyze the signal of the slope at $\beta=0.4$ and medium Q^2 ($\approx 10 \text{ GeV}^2$). If this signal is negative, then the dynamics of diffractive DIS is Regge based. On the other hand, if the signal is positive, a pQCD approach is necessary to describe the data; (ii) Second, to discriminate between saturated and non-saturated models, we can analyze the x_P of the slope at small values of β and medium Q^2 . While the non-saturated pQCD model predicts a steep growth at small values of x_P , the saturated model predicts an almost constant behavior. Of course, our results are dependent of the assumptions used in the models considered as input in the analyzes of the diffractive slope. However, we expect that the main point, the fact that this quantity is a potential observable to discriminate between the hard, semihard and soft dynamics, should not be modified by future theoretical improvements of the diffractive DIS.

We expect that our results could motivate the experimental analyzes of the logarithmic slope of the diffractive structure function in next years, since the behavior of this observable may explicit the dynamics in the small x regime.

ACKNOWLEDGEMENTS

MBGD acknowledges useful discussions with A. Capella, M. Derrick and E. Ferreira. VPBG thanks the FAPERGS and CNPq for support. MVTM acknowledges K. Golec-Biernat for useful enlightenments in the saturation model, as well M. Arneodo and P. Newman for comments on H1 and ZEUS data. This work was partially financed by CNPq and PRONEX (Programa de Apoio a Núcleos de Excelência), BRAZIL.

-
- [1] Yu. L. Dokshitzer. *Sov. Phys. JETP* **46**, 641 (1977); G. Altarelli and G. Parisi. *Nucl. Phys.* **B126**, 298 (1977); V. N. Gribov and L.N. Lipatov. *Sov. J. Nucl. Phys* **28**, 822 (1978).
 - [2] A. M. Cooper-Sarkar, R.C.E. Devenish and A. De Roeck, *Int. J. Mod. Phys* **A13**, 3385 (1998).
 - [3] M. B. Gay Ducati, V. P. Gonçalves, M. V. T. Machado. *Phys. Lett.* **B506**, 52 (2001).
 - [4] A. Caldwell, Invited talk, DESY Theory Workshop. DESY, Hamburg (Germany) October 1997. J. Breitweg *et al.*, *Eur. Phys. J.* **C7**, 609 (1999).
 - [5] H1 Collaboration. *Deep inelastic inclusive ep scattering at low x and a measurement of α_S* , [hep-ex/0012052] (to appear in *Eur. Phys. J. C*); ZEUS Collaboration. *A study of scaling violations in the proton structure function F_2* , in Conference ICHEP2000, [plenary session 12, paper 416];
 - [6] A. H. Mueller. *Small-x Physics, High Parton Densities and Parton Saturation in QCD*, in Proceedings of the NATO Advanced Study Institute on Particle Production Spanning MeV and TeV Energies, Nijmegen, The Netherlands, Edited by W. Kittel, P. J. Mulders and O. Scholten, p. 71. hep-ph/9911289.
 - [7] M. Glück, E. Reya, A. Vogt. *Eur. Phys. J.* **C5**, 461 (1998).
 - [8] A. D. Martin, R. G. Roberts, W. J. Stirling, R. S. Thorne. *Eur. Phys. J.* **C4**, 463 (1998).
 - [9] M. B. Gay Ducati, V. P. Gonçalves. *Phys. Lett.* **B487**, 110 (2000); Erratum-ibid. **B491**, 375 (2000); E. Gotsman *et al.* *Phys. Lett.* **B500**, 87 (2001).
 - [10] A.H. Mueller. *Eur. Phys. J.* **A1**, 19 (1999).
 - [11] A. Hebecker. *Phys. Rept.* **331**, 1 (2000).
 - [12] A. Capella *et al.* *Phys. Lett.* **B343**, 403 (1995).
 - [13] A. Capella *et al.* *Phys. Rev.* **D53**, 2309 (1996).
 - [14] J. Bartels, M. Wüsthoff. *J. Phys. G: Nucl. Part. Phys.* **22**, 929 (1996); J. Bartels *et al.* *Eur. Phys. J.* **C7**, 443 (1999).
 - [15] K. Golec-Biernat, M. Wüsthoff. *Phys. Rev.* **D59**, 014017 (1999); *Phys. Rev.* **D60**, 114023 (1999).
 - [16] G. Ingelman, P. Schlein. *Phys. Lett.* **B152**, 256 (1985).

- [17] A.B. Kaidalov, C. Merino, D. Pertermann. *Eur. Phys. J.* **C20**, 301 (2001).
- [18] A.B. Kaidalov, *Regge Poles in QCD*, [hep-ph/0103011].
- [19] A. D. Martin, M. Wüsthoff. *J. Phys. G: Nucl. Part. Phys.* **25**, R309 (1999).
- [20] A. Bialas, R. Peschansky, C. Royon, *Phys. Rev.* **D57**, 6899 (1998); M. Bertini et al. *Phys. Lett.* **B422**, 238 (1998).
- [21] L. V. Gribov, E. M. Levin, M. G. Ryskin. *Phys.Rep.* **100** (1983) 1; A. L. Ayala, M. B. Gay Ducati and E. Levin. *Nucl. Phys.* **B493**, 305 (1997), *idem* **B511**, 355 (1998); J. Jalilian-Marian *et al.* *Phys. Rev.* **D59**, 034007 (1999); Y. U. Kovchegov. *Phys Rev.* **D60**, 034008 (1999).
- [22] N. Nikolaev, B. G. Zakharov. *Z. Phys.* **C49**, 607 (1990).
- [23] J. R. Forshaw, D. A. Ross, *Quantum Chromodynamics and the Pomeron*, Cambridge University Press, 1997.
- [24] M. F. McDermott. *The dipole picture of small x physics (a summary of the Amirim meeting)*, hep-ph/0008260.
- [25] E. Levin. *Saturation at low x*, [hep-ph/0105205].
- [26] E. Gotsman et al. *Energy Dependence of σ^{DD}/σ_{tot} in DIS and Shadowing Corrections*, [hep-ph/0007261].
- [27] H1 Coll. *Z. Phys.* **C76**, 613 (1997); ZEUS Coll. *Eur. Phys. J.* **C1**, 81 (1998).
- [28] ZEUS Collaboration, *Measurement of the diffractive cross section at $Q^2 < 1 \text{ GeV}^2$ at HERA*, in 30th International Conference on High Energy Physics - ICHEP2000, Osaka, Japan (2000) [plenary session 12, paper 435].
- [29] A. Capella, E. G. Ferreira, A. B. Kaidalov, C. A. Salgado. *Nucl. Phys.* **B593**, 336 (2001); *Phys. Rev.* **D63**, 054010 (2001).

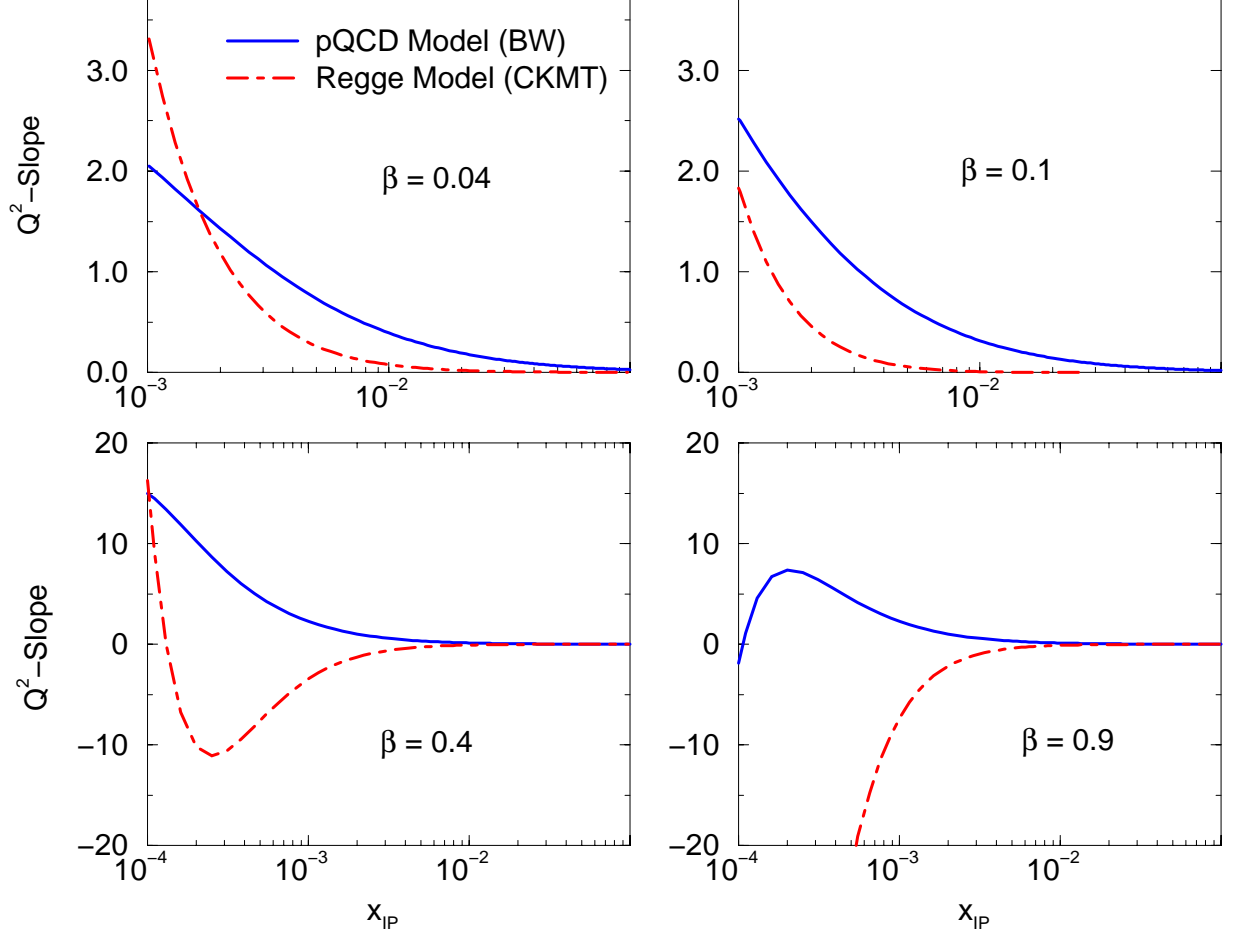


FIG. 1. The Q^2 -slope versus x_{IP} for the pQCD approach (solid lines) and Regge-CKMT (dot-dashed lines), at β typical values. We consider a kinematical constraint, $Q^2 = Q^2(x)$, taken from MRTS99.

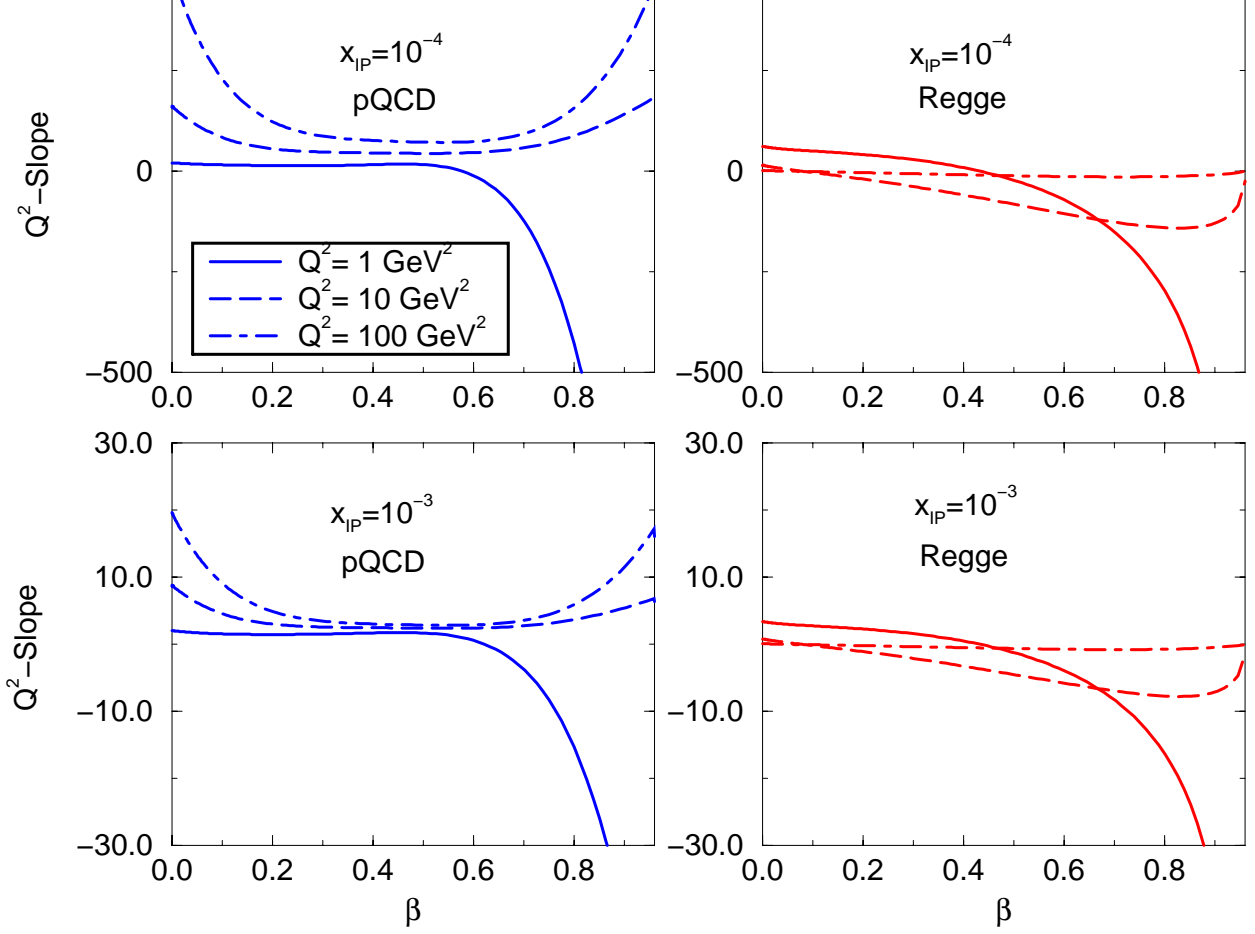


FIG. 2. The Q^2 -slope versus β for the pQCD approach (on the left) and CKMT model (on the right) without kinematical constraint. The graphs present the result for fixed x_{IP} and typical Q^2 values.

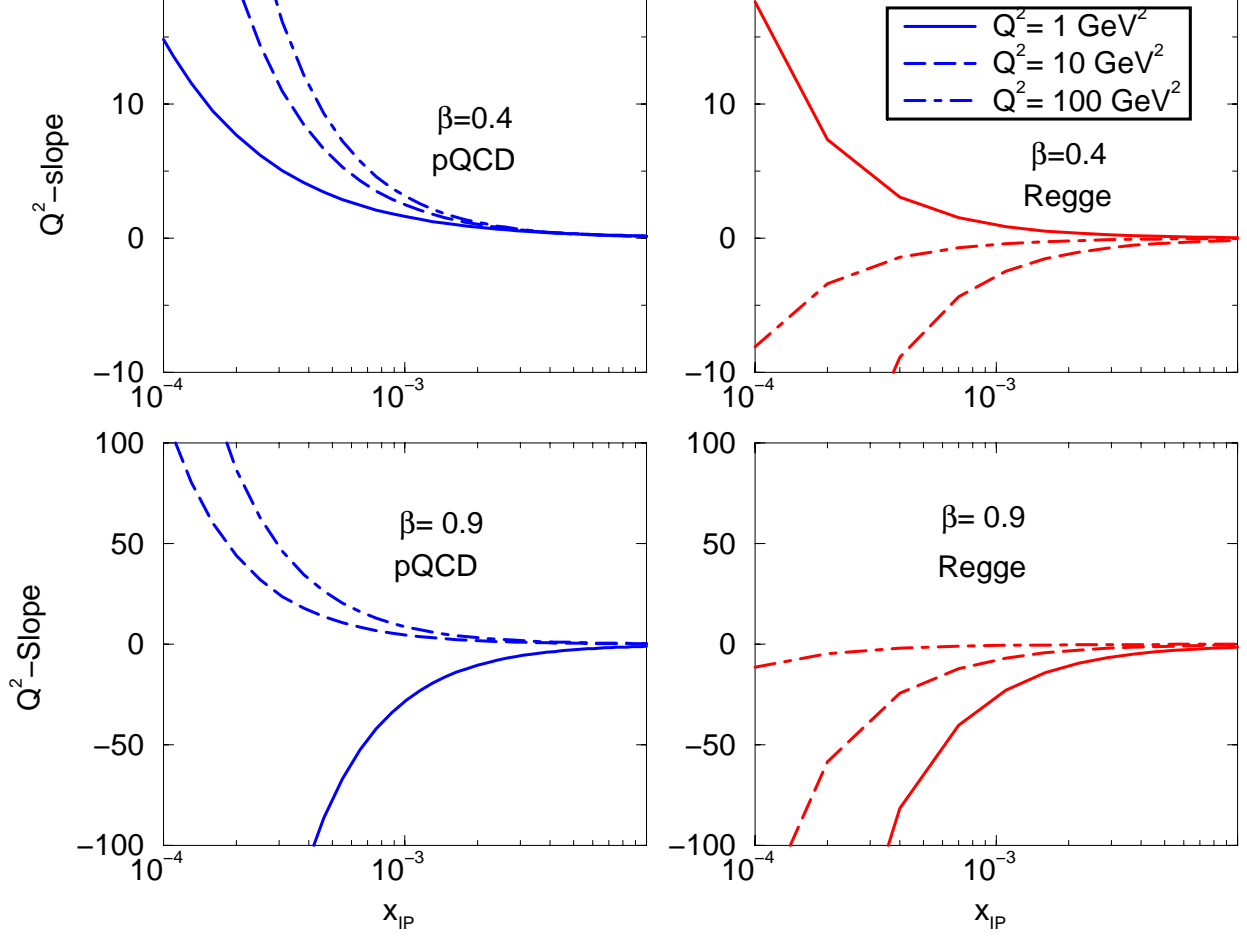


FIG. 3. The Q^2 -slope versus x_{IP} for the pQCD approach (on the left) and CKMT model (on the right) without kinematical constraint. The low β values were excluded to avoid the dominant reggeonic contribution in this region.

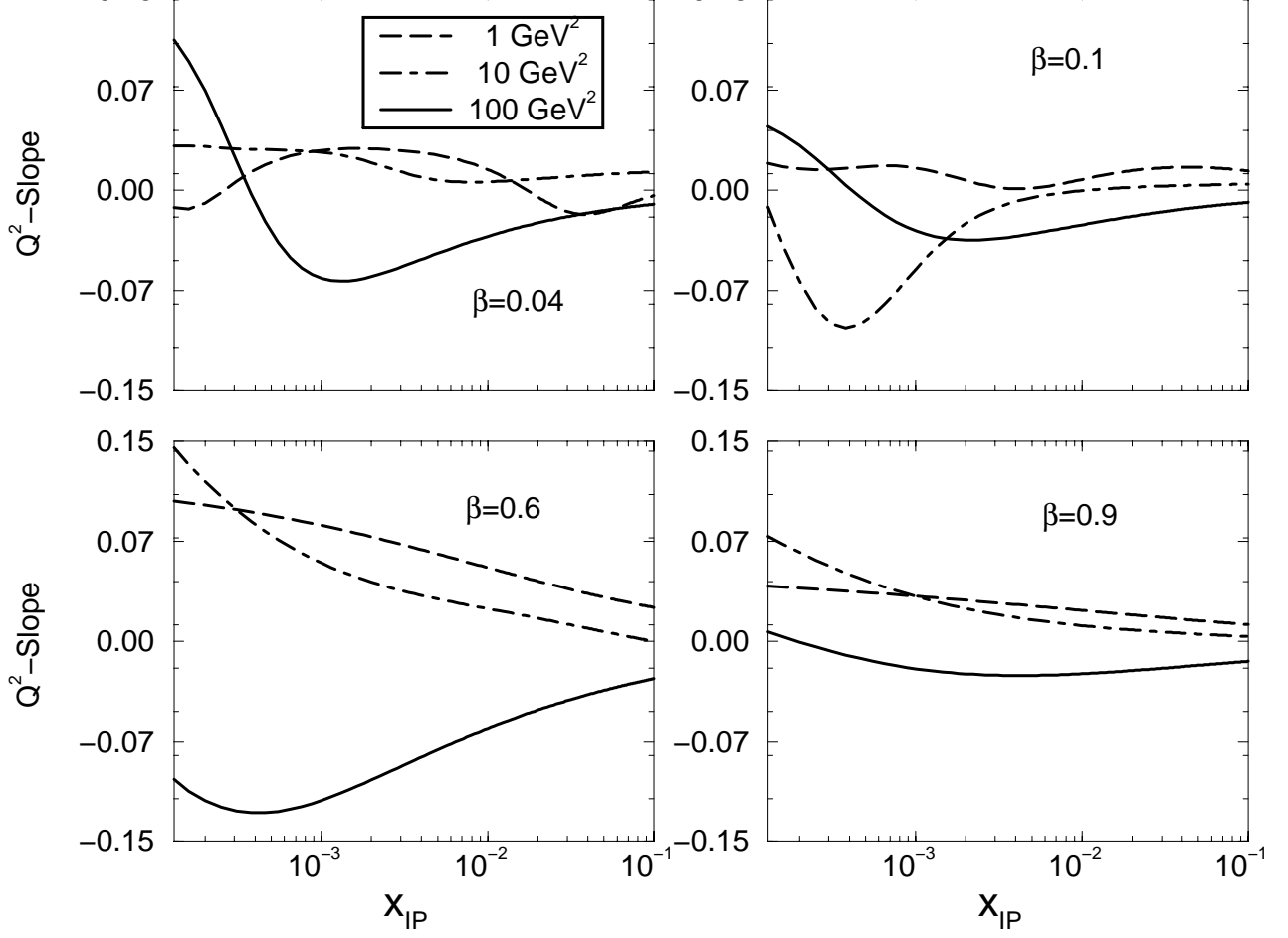


FIG. 4. The x_{IP} dependence of the logarithmic slope from the saturation model for the diffractive structure function, presented at typical β values. The analyzes is performed on photon momentum transfer Q^2 ranging from 1 up to 100 GeV^2 .

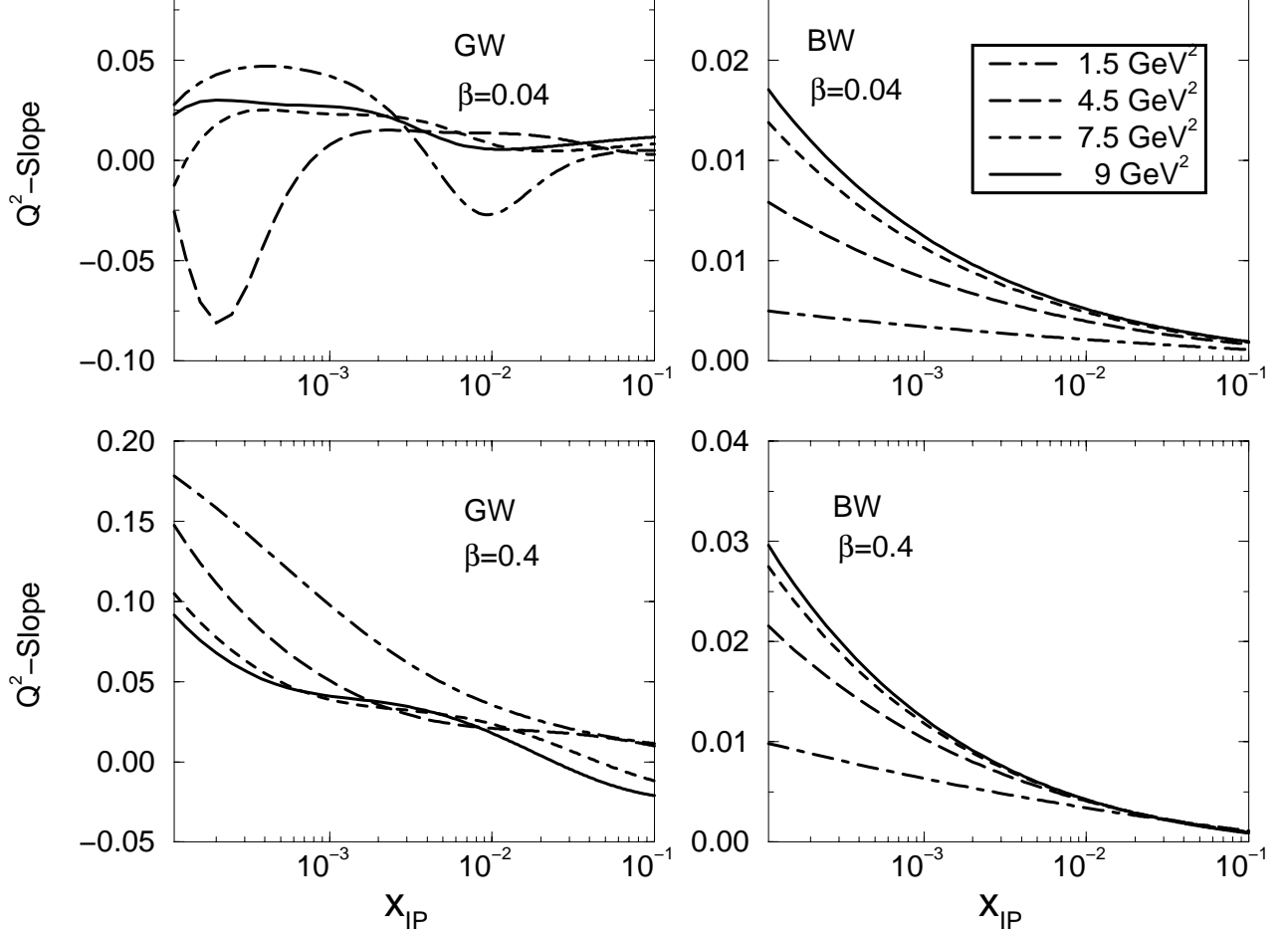


FIG. 5. The x_F dependence on the logarithmic slope from both Bartels-Wusthoff model (denoted BW, on the right) and the Golec Biernat-Wusthoff Saturation model (denoted GW, on the left), presented at typical β values. The analyzes is performed on low virtualities Q^2 ranging from 1.5 up to 9 GeV^2 .